

# FPGA based Hybrid Resonant Switching DC/DC converter for Electric Vehicles

Kanimozhi. G, Umayal. C, Dhanasekar.S

**Abstract:** A hybrid switching DC-DC converter for Hybrid Electric Vehicle with reduced on state conduction losses, voltage stress and switching losses of the power semiconductor devices is presented in this paper. Zero current switching and zero voltage switching is achieved for the leading and lagging legs of the inverter by using bipolar switching method. This reduces the circulatory losses in the transformer primary. Additionally it aids in exploiting the leakage inductance of the transformer to resonate with the output capacitor. Consequently this reduces the components count and the converter size. This results in efficient energy transfer as the inductive energy and capacitive energy acquired by the output inductor and resonant capacitor are simultaneously transferred to the load during the freewheeling interval. This boosts the converter efficiency when compared to the conventional converter. During active intervals, inductor is charged and the increased capacitor voltage is offered to the load. The bipolar circuit voltage is clamped during the freewheeling interval and reduces the peak voltage overshoots that crop up during the diode reverse bias period. Simulation for the DC-DC converter is rendered with PSpice software and the experimental results shows the desired output is achieved with reduced losses under variable load conditions.

**Index Terms:** Hybrid electric vehicles, DC/DC Resonant converters, battery chargers, Zero Voltage Switching, Zero Current Switching.

## I. INTRODUCTION

Generally a high voltage battery for powering the Plug-in hybrid electric vehicle [1,2] (PHEV) possess higher density to store energy in a way to drive electric traction system. Power factor correction at the supply point is also important which has isolated dc-dc converter next to it. Power factor correction helps in improving the quality of the input current and the dc voltage regulation. DC-DC converter is helpful in charging the high voltage pack. It also isolates the service mains from the traction battery pack.

The conventional phase shifted full bridge dc/dc converter is the prominent converter used as the second Interval of PHEV charger system. Zero Voltage Switching (ZVS) can also be realized by exploiting the parasitic capacitance of the switches as well as the leakage inductance of the transformer. Conventional converter has many limitations in achieving ZVS for wide voltage range [3-7]. The range of ZVS of lagging leg inverter switches is found to be limited. Resonance is achieved from half to full load condition. Voltage across leakage inductor ( $l_k$ ) is responsible for

achieving ZVS in lagging – leg switches however this condition fails when load conditions are low.

To overcome the above problem, the values of the leakage inductance can be increased or a serial inductor can be added externally. Adding a higher value inductance may introduce a delay in the primary current. This delay may further lead to loss in the transformer secondary. To compensate these losses, a transformer with higher turn's ratio must be employed. But this results in high voltage stress for the switches in bridge rectifier. A number of methods are reported in the literature for exploiting the inductive energy accumulated in supplementary circuits, instead of adding external series inductance to increase the ZVS range [5,6]. Three major drawbacks of conventional methods are as follows: First, the batteries of electric vehicle applications may require wide range of load and duty cycle. ZVS cannot be attained at wider range. Secondly, the primary current on the primary part circulates during freewheeling period. This contributes to unnecessary conduction losses. The third major drawback is the voltage overshoot across the diodes in the output side. This is due to parasitic ringing occurs in the junction capacitors and also in transformer leakage inductance. RCD[7] snubber circuits are used to reduce voltage overshoots in the bridge rectifier. But this increases the losses and decreases the converter efficiency. However solving this problem intensifies the complexity and reduces the system reliability. Several clamp circuits with effective passive components are proposed [8,9]. Though these techniques are able to give a solution for reducing the voltage stress, the value of these voltage stress rely on the duty cycle in addition to the output voltage value [10-12]. Therefore, these techniques were commonly not considered for battery charger circuit's applications.

## II. HYBRID SWITCHING RESONANT DC-DC CONVERTER

Fig.1 shows the proposed circuitry for hybrid switching resonant DC-DC converter. It consists of an inverter having a higher frequency with reduced voltage ripple at the load end and also includes four switches ( $S_1 - S_4$ ) connected to the isolation transformer primary end and diode bridge rectifier on secondary end for synchronous rectification. This topology employs ZVS for the four switches which lead to a diminished switching losses and higher converter efficiency. Switches ( $S_1, S_2, S_3$  and  $S_4$ ) operate in pairs, hence the term bipolar. The switches  $S_1/S_2$  are considered as leading leg pair and  $S_3/S_4$  as switches at the lagging leg. ZVS of the leading leg can be attained using transformer leakage

Revised Manuscript Received on July 05, 2019

Kanimozhi.G, School of Electrical Engineering, Vellore Institute of Technology, Chennai, Tamil nadu, India

Umayal.C. School of Electrical Engineering, Vellore Institute of Technology, Chennai, Tamil nadu, India

Dhanasekar.S, School of Advanced Sciences, Vellore Institute of Technology, Chennai, Tamil nadu, India

inductance. However, since the ZVS in lagging leg switches  $S_3$  and  $S_4$  is attained using energy accumulation in leakage inductance of the transformer, it fails to accomplish ZVS [13,14] under low load conditions.

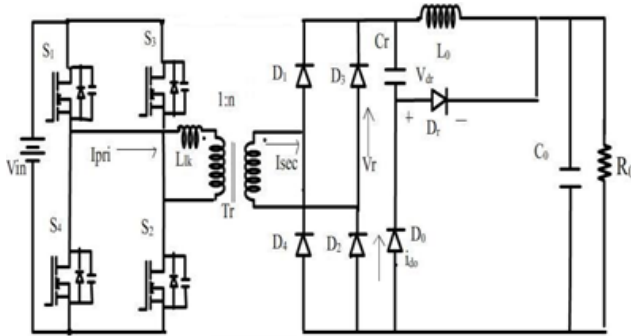


Fig.1 Proposed resonant dc/dc converter

Hybrid resonant waveforms and pulse width modulated current waveforms are used to examine the resonant converter. During active intervals, the energy gets discharged from the input supply to the load along a resonant path via transformer. This enhances the power transfer from input power supply to load. All along the freewheeling period, the accumulated energy in the resonant path will be sent to the load. Fig.1 depicts the proposed converter which provides an additional circulating current which in turn forces the primary current to zero at the beginning of freewheeling period. It should be noted that, during this interval the voltage across  $C_r$  is the same as the voltage across the uncontrolled converter. This decreases the voltage stress (dv/dt) across the rectifiers. The working principle of the classical DC-DC converter relies on the stored inductive energy [15] whereas the proposed converter has an added capacitive energy transmitted to the output by hybrid switching method. The circulating current is nonexistent for the period of the freewheeling interval [16-19].

### III. DETAILED OPERATION OF HYBRID SWITCHING RESONANT CONVERTER

The converter function is reviewed with the aid of three operational modes:

a. Mode 1: The resonant current that passes through the diode  $D_r$  ( $I_{dr}$ ) forms the basis for the classification of Mode 1 into six topological Intervals. Fig 2 depicts the waveforms for different Intervals of Mode 1. The voltages in the primary and secondary part of the transformer are  $V_{pri}$  and  $V_{sec}$ ;  $i_{pri}$  and  $i_{sec}$  are the current flowing through transformer primary and secondary end.  $i_{Lo}$  represents output inductor current and it is higher than  $i_{sec}$  as shown in the figure 2.

**Interval 1:** [Fig 3(a)]. Interval 1 starts before  $t_1$ . During this period, the currents flowing through both primary and secondary windings are zero. Resonant capacitor  $C_r$  turns off the bridge rectifier diodes by applying reverse voltage. The stored energy in the resonant capacitor is released through diode  $D_0$  and inductor  $L_o$ . At time  $t_1$ , switch  $S_2$  turns ON. As a result, the primary and secondary currents of the transformer increase. This mode changes once the secondary end current  $I_s$  is higher than the inductor current ( $i_{Lo}$ ) at the output.

**Interval 2:** This interval starts when the secondary end current

is greater than the output inductor current which turns ON diode  $D_r$  and brings  $D_0$  under reverse bias condition. The Interval 2 operation of mode1 is shown in Fig.3(b). This result in an increase in the power delivered to output, because the energy transferred is the parallel combination of sinusoidal resonant mode and linear PWM modes.

$$Tr = n.(ilo + idr) \quad (1)$$

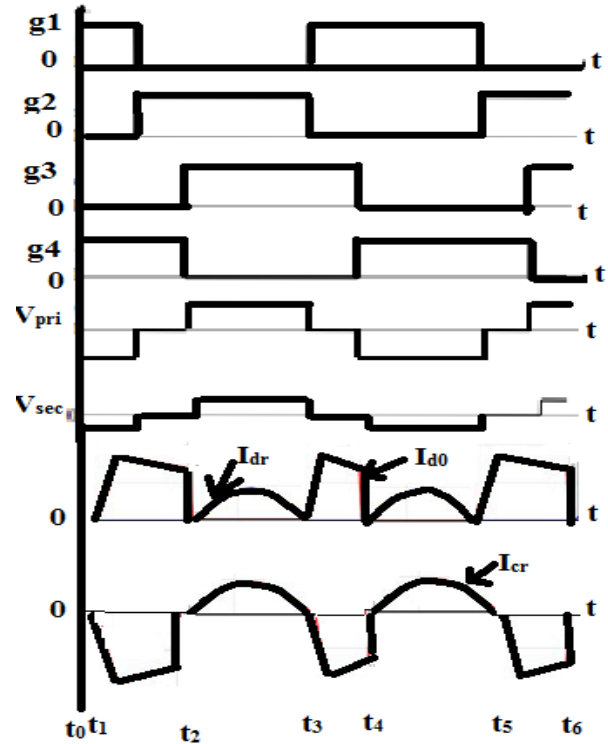


Fig.2 Converter Waveforms (Theoretical)

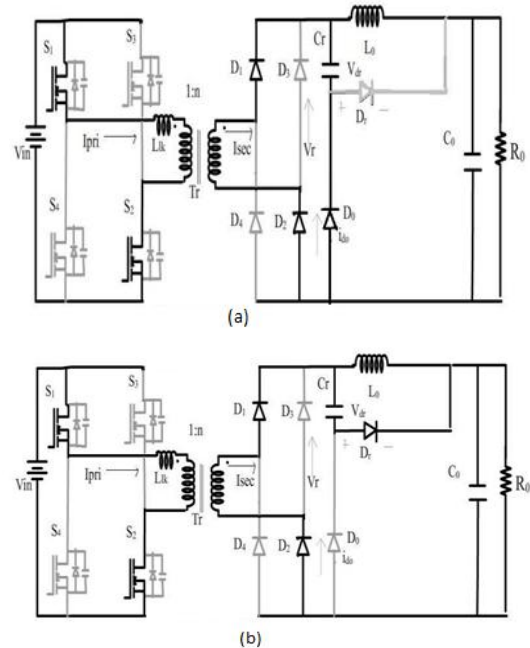
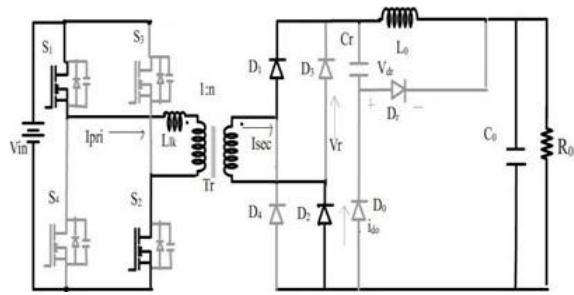
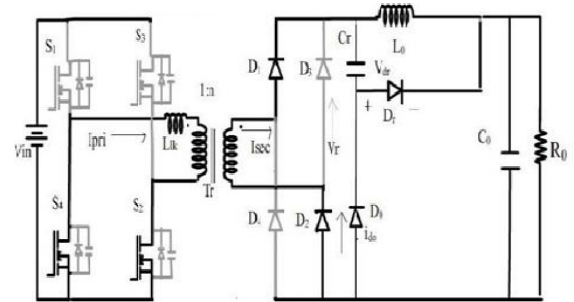


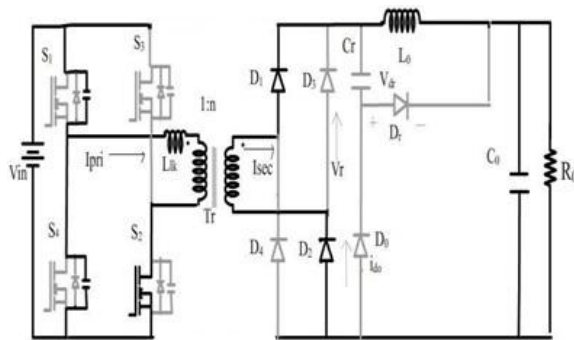
Fig.3 Topological intervals of Mode 1 (a) Interval 1  
(b) Interval 2



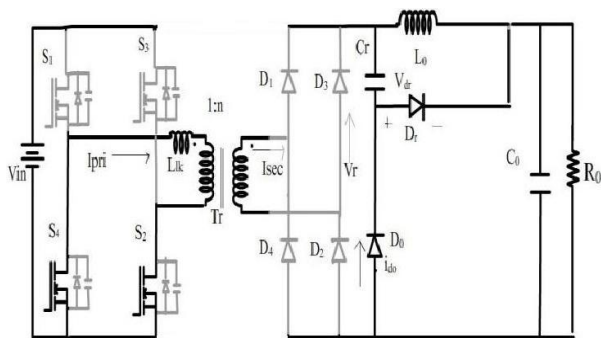
(c)



(d)



(e)



(f)

Fig 4. Mode 1 operation (c) Interval 3 (d) Interval 4 (e) Interval 5 (f) Interval 6

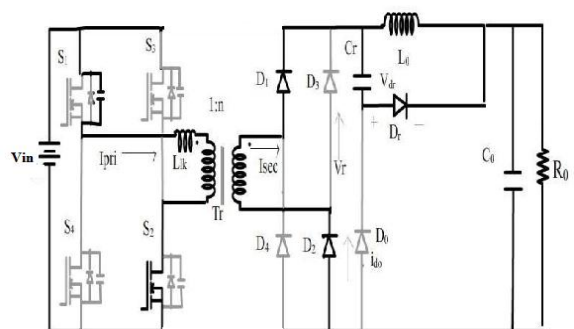


Fig.5 Mode 3 operation

*Interval 3:* Interval 3 operation of mode 1 starts at time instant  $t_2$  as represented in Fig.4(c). The diode current ( $I_{dr}$ ) resonates to zero at time instant  $t_2$ . The stored energy in transformer windings are dissipated to load until the current through the secondary equals to  $I_{lo}$ .

*Interval 4:* [Fig 4(d)]. In this interval the switch  $S_1$  remains off and the transformer primary current ( $i_{pri}$ ) charges and discharges the junction capacitance of switch  $S_3$ . As the drain– source voltage ( $V_{ds3}$ ) of switch  $S_3$  attains zero,  $i_{pri}$  flows through the  $S_3$  body diode and once the dead time passes,  $S_4$  is turned ON with ZVS.

*Interval 5:* [Fig 4(e)]. Secondary side current is lesser compared to  $I_{lo}$ , which in turn brings the diode  $D_0$  under forward bias condition. The voltage across the bridge rectifier matches the capacitor voltage ( $V_{cr}$ ). Thus the primary current becomes zero turning off  $S_1$  and  $S_3$ .

*Interval 6:* [Fig 4(f)]. Currents flowing in through the transformer turns are zero. Stored energy in  $C_r$  and  $L_o$  is dissipated to the load, until  $S_4$  switch is turned ON. The bridge rectifier is under reverse bias condition as the resonant capacitor ( $C_r$ ) voltage is usually more than zero.

b. Mode 2: The operation of Mode 2 is analogous to the previous mode. The variation in Mode 2 occurs when the resonant current  $I_{dr}$  approaches zero and switch  $S_1$  turns OFF.

c. Mode 3 [Fig 5]: In mode 3, resonant diode current is more than zero. When converter operates in freewheeling period, resonance halts and Switch  $S_1$  is turned OFF. Primary current comprises of the resonant diode current and the current at the output inductor. As the current flowing through  $S_3$  approaches zero, charging and discharging of the junction capacitor occurs. Primary current flows through body diode once  $S_1$  and  $S_3$  are in OFF state. The following equation is obtained after making use of flux balance condition for inductor:

$$VC_r * Dr + (nVin - Vo) * (D - Dr) + (1 - D) * (Vo - Vcr) \quad (2)$$

#### IV. HYBRID SWITCHING RESONANT DC / DC CONVERTER CHARACTERISTICS:

In the conventional converter during active period, the voltage drop occurs across two diodes in the bridge rectifier whereas in the suggested topology the voltage drop is only across one diode. This is due to the voltage drop across  $C_r$  (resonant capacitor) is greater than zero. Fast recovery diode has an advantage of high rate of commutation and less reverse recovery current. As the transformer secondary voltage is high, a large voltage drop occurs across the diode bridge rectifier which might cause higher conduction losses. But this does not alleviate the diodes reverse recovery problem and can be resolved by considering the transformers leakage inductance. The energy is stored in  $C_r$  and  $L_o$ , when the energy transfer occurs between the supply and the load. During the freewheeling period this energy is transferred to the load. This provides additional current to ZVS and sets the primary current to zero during the



start of freewheeling period. Hence switches at the leading leg can realize ZVS for an extensive power range. The suggested converter is more efficient than ZVS converter [16]. By employing ZVS and PWM control switching losses are significantly reduced.

## V. DESIGN CONSIDERATIONS

This converter has constant ON-time and matches half the resonant period. The OFF-time is controlled. The ON-time equation is obtained as

$$T_{on} = D.T_s = \frac{T_r}{2} = \pi C_r \sqrt{L_r} \quad (3)$$

Since the transformer leakage inductance is used to attain resonance,  $L_r$  is substituted with  $L_{lk}$ . Resonant time period is

$$T_r = 2\pi C_r L_{lk} \quad (4)$$

To attain resonance, the dead time required among the switches  $S_1$  and  $S_4$  can be obtained by the following expression:

$$C_{s1} + C_{s4}.V_{in} + CTr \leq I_{pri} \cdot \delta t_1 \quad (5)$$

where  $t_1$  is  $S_1$  and  $S_4$  dead time. The design equations of the transformer are given by

$$\frac{N_1}{N_2} = \frac{V_1}{V_2} \sqrt{\frac{I_1}{I_2}} \quad (6)$$

$$\frac{I_1}{I_2} = \frac{\mu N_1 \pi r^2}{\mu N_2 \pi r^2} \quad (7)$$

The peak ripple current equation is given by

$$\Delta i_{2pk} = \frac{\left(\frac{1}{nM} - 1\right) \left(2 - \frac{1}{nM}\right) \cdot V_o \frac{t_s}{2}}{L_o} \quad (8)$$

Where  $M = \frac{V_o}{V_{in}} = \frac{1}{2-D}$  and  $M$  represents conversion ratio and  $n$  represents turns ratio of the transformer. The inductor current comprises of the diode current  $D_r$  and capacitor resonant current through  $C_r$ . Hence resonant capacitor charge balance equation is given by the condition that the resonant capacitor

voltage must be greater than zero and is should satisfy the following equation:

$$v_{cr} < V_{Cr} \quad (9)$$

The critical value of the capacitance is given by

$$C_r \gg \frac{(2-D).P_o}{8 \cdot n^2 \cdot V_{in}^2 \cdot f} \quad (10)$$

Where  $P_o$  represents the load power and  $V_{in}$  is the input voltage of the converter. The resonant capacitor current  $i_{cr}$  is expressed as

$$i_{cr} = (1-d) i_o \quad (11)$$

where  $i_o$  is the current through the inductor.

## VI. SIMULATION RESULTS

Converter design parameters are given in Table 1. The dead time is given for the triggering pulses of switches from  $S_1$  to  $S_4$  to accomplish ZVS as illustrated in Fig.6 (a). The drain source voltage ( $V_{ds1}$ ,  $V_{ds2}$ ,  $V_{ds3}$  and  $V_{ds4}$ ) of inverter switches are given in Fig.6 (b). The voltage across the transformer primary and secondary can be noticed in Fig 6(c). The bridge rectifier voltage stress is almost identical to the secondary voltage of the transformer and hence only one voltage drop during the freewheeling interval. The load current  $I_o$  and inductor current ( $I_{Lo}$ ) are depicted in Fig 6(d).



Fig.6 (a) Triggering pulses of four switches (S1- S4)

From the Fig 6(f) it can be observed that the inductor current at the load end is the addition of the current through the resonant capacitor  $C_r$  and the diode. Fig.7 reveals that the converter's operating range is obtained at a duty cycle of 0.45.

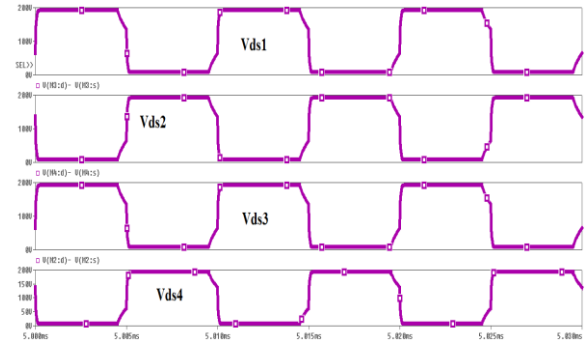


Fig.6(b) Drain source voltage ( $V_{ds}$ ) of the four switches

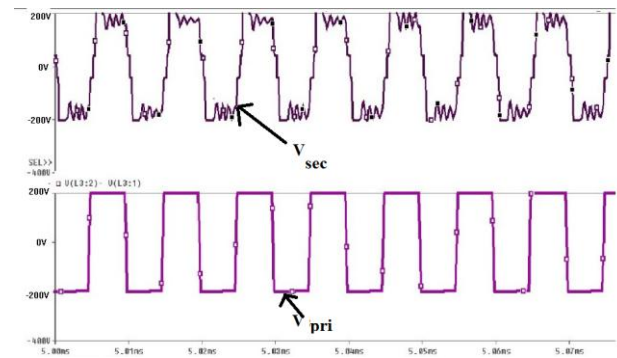


Fig.6(c) Transformer secondary and primary winding voltage

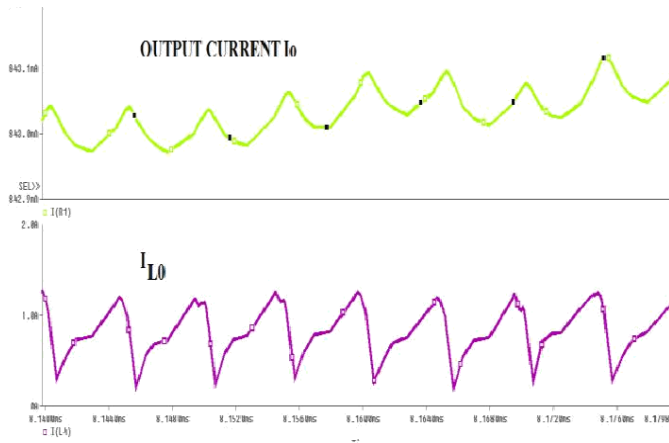


Fig 6(d) Load current and the current through the inductor  $L_o$

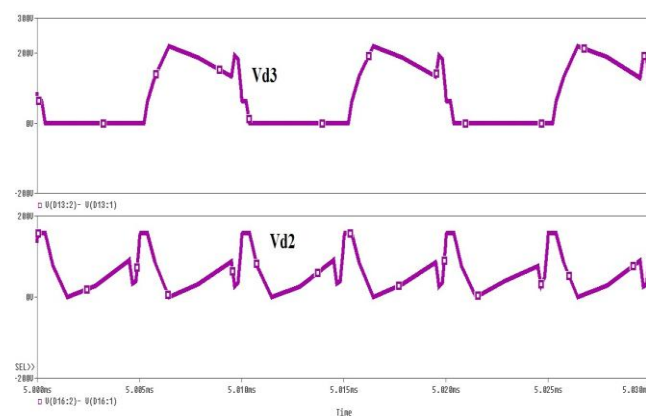


Fig.6 (e) Voltage across the uncontrolled converter

## VII. HARDWARE RESULTS

A 50W experimental model is realized to validate the performance of hybrid resonant DC/DC converter. Hardware specifications are listed in Table.2 with an isolation transformer. Secondary of the transformer is coupled to the diode bridge rectifier (DBR) which consists of schottky diodes.

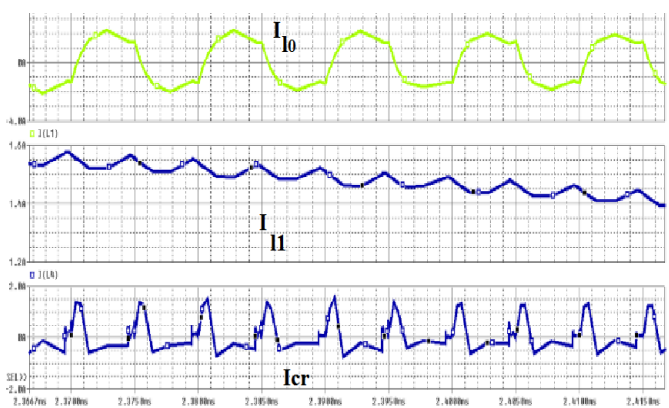


Fig. 6(f) Waveforms illustrate inductor current, primary current through the transformer and resonant capacitor current

Table 1: Converter Parameters

Parameter	Value
Input dc voltage	200V
Output load voltage	175V
Power rating	100W
Resonant capacitor (	470 nF
$C_r$	
Output inductor (	270mH
$L_o$	
Output capacitor(	47uF
$C_o$	
Diodes	MUR1560
$(D_1, D_2, D_3, D_4, D_r)$	

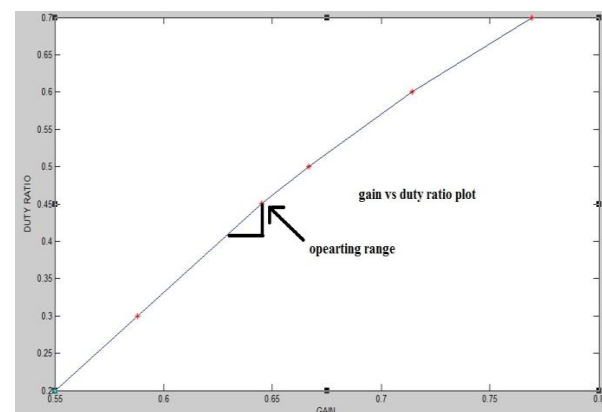
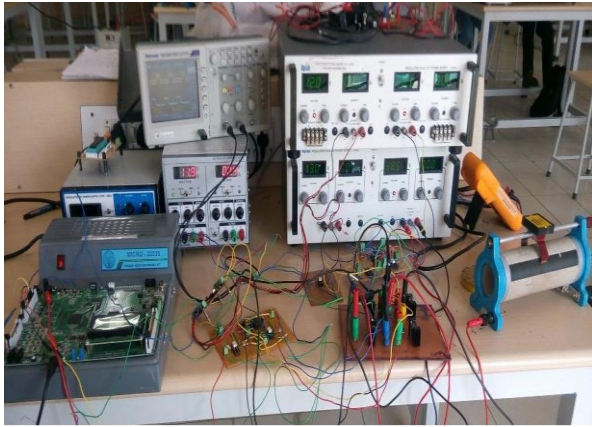


Fig.7 Gain Vs Duty ratio

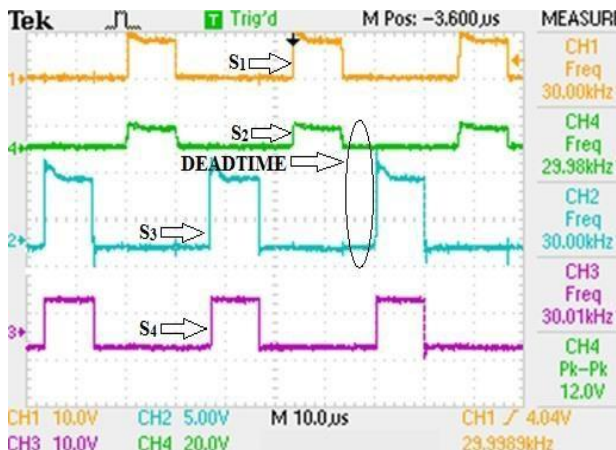
This rectifies the voltage at the input for the full bridge converter. The resonant part which contains a resonant diode, inductor and the capacitor of the topology is used to attain the zero voltage switching for the proposed converter. To generate the pulses for the proposed converter Spartan –6 XC6SLX25 FPGA board is employed. PWM output from FPGA is terminated in a 34 Pin connector through Level Translator for converting 3.3V to 5V. There are 8 pins to generate PWM pulses. FPGA board has a clock frequency of 100MHz. By dividing this internal clock frequency the desired switching frequency can be obtained. Figure 9(a) illustrates the experimental setup of the proposed converter.

Table 2 Converter Specifications

Symbol	Parameter	Value
P0	Power rating	50W
$V_{in}$	Input voltage	100VDC
VOUT	Output voltage	65VDC
$f_s$	Switching frequency	30kHz
$I_{max}$	Max current	2A
$L_r$	Resonant inductor	2.7 mH
$C_o$	Output capacitor	47uF/150v
$C_r$	Resonant capacitor	0.47uF/150V (polypropylene)
$T_r$	Transformer turns ratio	(39:24) ( $V_1/L_1$ :150/4mH) ( $V_2/L_2$ :100/3.1mH)
$S_1, S_2, S_3, S_4$	Switches	IRF740
$D_1, D_2, D_3, D_4, D_r$	Diode	MUR1560 (schottky diodes)



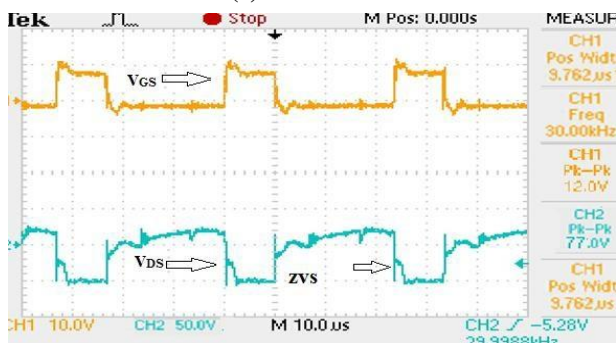
(a)



(b)



(c)



(d)

**Fig 8(a) Hardware test bench (b) Gate pulses of High Side and Low side switches with  $f_s=30\text{kHz}$  (c) Current across the resonant inductor (d) Waveform showing ZV switching across diode.**

Figure 8(b) shows the pulses generated with the dead time. From the figure it could be seen that switches  $S_1$  and  $S_2$  are working with a phase shift of  $180^\circ$  between them. Dead time of  $770\text{ns}$  can be observed between  $S_1$  and  $S_2$ . The resonant inductor current is shown in Fig.8(c) and Fig 8(d) depicts the zero voltage switching of diode. The output voltage as well as the current through the resistive load is shown in Fig.9 with a magnitude of  $41.3\text{V}$  and  $1.64\text{A}$ .



**Fig 9 The load voltage and load current waveforms**

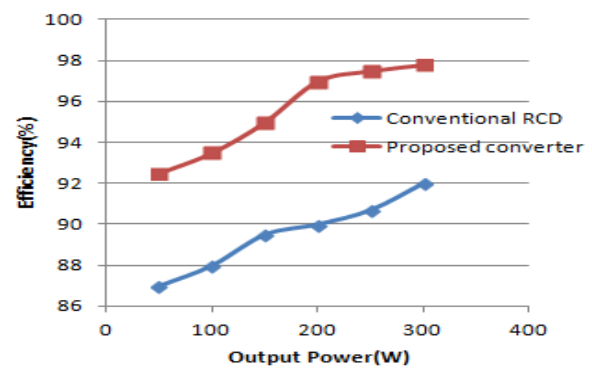


**Fig.10 Efficiency Vs Output power**

## VIII. CONCLUSION

This paper discusses a hybrid switching resonant converter for hybrid electric vehicle applications. Zero Voltage Switching of inverter switches can be attained at variable load condition. Thus the soft switching technique eliminates the overall converter losses. The transformer leakage inductance is used to resonate along with output inductor and hence a supplementary component for achieving resonance is reduced. Since the hybrid switching resonant converter is operated at higher switching frequencies, the cost and size of the passive circuit elements are reduced. This results in overall converter size reduction and increases the converter efficiency.

## REFERENCES:

1. K.Morrow; D. Karner and J. Francfort, "Plug-in hybrid electric vehicle charging infrastructure review", *Vehicle Technologies Program*. U.S. Department of Energy, Washington- DC, 2008.
2. C.A.Bendall and W.A.Peterson, "An EV on-board charger," *Proceedings of the IEEE Applied Power Electronics Conference*. Feb 1996, pp 26–31.
3. H. Bai and C.C. Mi, "Comparison and evaluation of different DC/DC topologies for plug-in hybrid electric vehicle chargers" *International Journal of Power Electronics*, Vol.4(2),2012,pp 119–133.



4. J. A. Sabate; V. Vlatkovic; R. B. Ridley; F. C. Lee; and B. H. Cho, "Design considerations for high-voltage high-power full-bridge zero-voltage switched PWM converter", *Proceedings of the IEEE Applied Power Electronics Conference*. 1990, pp-275–284.
5. Y. Jang; M.M. Jovanovic, and Y. M. Chang, "A new ZVS-PWM full bridge converter," *IEEE Trans. Power Electronics*, Vol. 18(5), 2003, pp 1122– 1129.
6. L.H. Mweene; C.A. Wright; and M.F. Schlecht, "A 1 kW 500 kHz front-end converter for a distributed power supply system", *IEEE Trans. Power Electronics*, Jul,6(3),1991,pp 398–407.
7. R. Redl; N.O. Sokal, and L.Balogh, "A novel soft-switching full-bridge DC/DC converter: Analysis, design considerations, and experimental results at 1.5 kW, 100 kHz", *IEEE Transactions on Power Electronics*. Jul, 6(3),1991,pp 408–418.
8. J.G. Cho; J.W. Baek; C.Y. Jeong and G.-H. Rim, "Novel zero-voltage and zero current switching full-bridge PWM converter using a simple auxiliary circuit," *IEEE Transactions Industrial Applications*. Feb, 35(1), 1999 pp 15–20.
9. E.S.Kim and Y.H. Kim, "A ZVZCS PWM FB DC/DC converter using modified energy-recovery snubber", *IEEE Transactions on Industrial Electronics*. Oct, 49(5), 2001,pp 1120–1127.
10. X. Wu; X. Xie; J. Zhang, R. Zhao; and Z. Qian, "Soft switched full Bridge dc-dc converter with reduced circulating loss and filter requirement", *IEEE Transactions on Power Electronics*. Sep,22(5), 2007, pp 1949–1955.
11. T. Song and N. Huang, "A novel zero-voltage and zero-current switching full bridge PWM converter", *IEEE Transactions on Power Electronics*. Mar, 20(2), 2005,pp 286–291.
12. A. Bendre; S. Norris; D. Divan; I. Wallace, and R. W. Gascoigne (2003). New high power dc-dc converter with loss limited switching and lossless secondary clamp. *IEEE Transactions on Power Electronics*. Jul,18(4), pp 1020–1027.
13. S. Moiseev; K. Soshin and M. Nakaoka, "Tapped – inductor filter assisted soft switching PWM dc-dc power converter", *IEEE Transactions on Aerospace and Electronic Systems*. Vol. 41(1),2009, pp 174–179.
14. Y. Jang; M.M. Jovanovich and Y. M. Chang , "A new ZVS PWM full bridge DC-DC converter. *IEEE Transactions on Power Electronics*. Vol.18 (5), 2005, pp 1122–1129.
15. P.K. Jain; W. Kang, H. Soin, and Y.Xi, "Analysis and design considerations of a load and line independent zero voltage switching full bridge dc- dc converter topology", *IEEE Transactions on Power Electronics*. Vol.17 (5), 2002, pp 649– 650.
16. Shriniketh C.M and Kanimozhi G," Implementation of ZVS in an interleaved boost rectifier", *International Journal of Applied Engineering Research*, Vol. 10 No.20 (2015), pp 15852-15857.
17. K.Likhitha; Kumar S.S and G Kanimozhi, "Isolated DC-DC zero voltage switching converter for battery charging applications," *Proceedings of Biennial International Conference on Power and Energy Systems: Towards Sustainable Energy (PESTSE)*. 2016,pp-1-5.
18. G Kanimozhi; S Sathish Kumar and K Likhitha, " Battery charger for automotive applications" *IEEE proceedings of 10th International Conference on Intelligent Systems and Control (ISCO)*. India, pp 1-6.
19. Jaisudha S., Sowmiya Srinivasan, Kanimozhi G, "Bidirectional Resonant DC-DC converter for Microgrid Applications," *International Journal of Power Electronics and Drives Systems*, Vol.8, No.4, Dec 2017, pp- 1548-1561.



**Dhanasekar S** received his PhD from Bharathiyar University. He is working as Assistant Professor in the School of Advanced Sciences, VIT Chennai, India. He has authored many international and national level research papers on Fuzzy optimization.

## AUTHORS PROFILE



**Kanimozhi.G** received her Bachelor of Engineering from Bharathiyar University, Master of Engineering from Anna university and her Ph.D from VIT University, Chennai. She is working as Assistant Professor (Selection Grade) in the School of Electrical Engineering, VIT Chennai. Her research area includes AC-DC converters for Electric vehicles, Electromagnetics, Multilevel inverters and DC-DC resonant converters.



**Umayal.C**, received her Bachelor of Engineering from University of Madras, Master of Engineering and Ph.D from Anna University. She is working as Associate professor in the School of Electrical Engineering, VIT, Chennai, India. She has authored many international and national level research papers on power factor correction in PMBLDC Drives.